DReAM: Demand Response Architecture for Multi-level District Heating and Cooling Networks

Saptarshi Bhattacharya[1], Vikas Chandan[2], Vijay Arya[3] and Koushik Kar[1]
[1]Rensselaer Polytechnic Institute, Troy, NY, USA,
[2]Pacific Northwest National Laboratory, Richland, WA, USA,
[3]IBM Research, India.
bhatts5@rpi.edu,vikas.chandan@pnnl.gov,vijay.arya@in.ibm.com,koushik@ecse.rpi.edu

ABSTRACT

In this paper, we exploit the inherent hierarchy of heat exchangers in District Heating and Cooling (DHC) networks and propose DReAM, a novel Demand Response (DR) architecture for Multi-level DHC networks. DReAM serves to economize system operation while still respecting comfort requirements of individual consumers. Contrary to many present day DR schemes that work on a consumer level granularity, DReAM works at a level of hierarchy above buildings, i.e. substations that supply heat to a group of buildings. This improves the overall DR scalability and reduce the computational complexity. In the first step of the proposed approach, mathematical models of individual substations and their downstream networks are abstracted into appropriately constructed low-complexity structural forms. In the second step, this abstracted information is employed by the utility to perform DR optimization that determines the optimal heat inflow to individual substations rather than buildings, in order to achieve the targeted objectives across the network. We validate the proposed DReAM framework through experimental results under different scenarios on a test network.

KEYWORDS

District Heating and Cooling Networks, Demand Response, Energy cost optimization

1 INTRODUCTION

District Heating and Cooling (DHC) networks are fast emerging as a major component of sustainable energy systems worldwide [15], [14], [17]. Also known as thermal grids, DHC networks are complex interconnections of buildings wherein a heated fluid (typically hot water) is piped from a central source to the connected buildings to meet their space heating and hot water requirements. DHC networks are frequently seen in several European countries (especially countries like Sweden, Finland and Denmark) where almost 62 million consumers are served through them, totaling about 12% of the entire population [1]. These networks are also popular in several parts of the United States. For example, the utility company Consolidated Edison (ConEd) serves a major section of Manhattan through district heating [3].

In the context of operation of these thermal grids, extreme weather conditions may cause a surge in energy demand for space heating in which case DHC networks must secure additional energy from uneconomical sources (such as fossil fuel based peak firing plants) to cater to the increasing demand. For the utility company in charge of DHC network operations, it may then be economical if the end-consumer load can be somehow controlled through central coordination. On the other hand, at the building level, each consumer typically has a comfort range of its own, breaching which may lead to consumer discomfort and disgruntlement in the long run. Thus, the central utility company in charge of DHC operations is faced with the task of coordinating the downstream consumer load which in turn would tune the energy expenditure at the central heat source through appropriate *Demand Response (DR)* algorithms.

DHC networks typically can be segregated into two distinct levels from an operational standpoint. Usually, the first level is a *primary network* of pipes feeding hot water from a central energy source to the individual *substations*. In the second level, the energy is channelized from the substations through a *secondary network* (which is physically decoupled from the primary network) to individual buildings under the substations. In several cases, the total number of buildings (consumers) served by a DHC network can be quite large. For example, in Lulea, Sweden, more than 50,000 consumers are served by a DHC network. In order to optimize the system wide operation, the utility ideally should be cognizant of the necessary parameters of all such individual buildings and the respective comfort preferences of their consumers. This *network knowledge discovery* step is invariably resource intensive, has very high communication overhead and frequent implementation of this step in any energy management algorithm reduces its practical merit. Also, performing the DR at a building level by centrally tuning the individual set-points may become computationally intractable for the central utility.

In this paper, we design a hierarchical DR architecture named **DReAM** (**D**emand **Re**sponse **A**rchitectute for **M**ulti-level DHC networks) that can facilitate economic operation (in general, it may optimize any generic social welfare metric) in a DHC network, while being cognizant and respectful of the comfort requirements of end-consumers. In DReAM, we first limit the laborious network knowledge discovery stage to a one time event. We then employ this acquired knowledge over the entire horizon of network operation to centrally optimize the desired network wide performance metric over a decision space with reduced dimensionality. This

e-Energy '17, Shatin, Hong Kong

DOI: http://dx.doi.org/10.1145/3077839.3084079

makes it computationally less complex than a case where DR is performed at the building level. At present, DHC network utilities mostly resort to simple heuristic techniques, devised and perfected through brute force experimentation, in order to bring about energy (cost) savings at the central energy source. In the wake of ever-advancing information and communication technologies, DReAM can serve as a blueprint for DHC utility companies to carry out energy management in DHC networks in a computationally efficient and optimal manner.

1.1 Related Work

Researchers have taken several approaches to deal with the issue of energy management in thermal grids in order to achieve targeted network objectives such as peak reduction and cost optimization. Some of these approaches focused on controlling the mass flow rates of water within the network appropriately to optimize pumping and heat losses [8], cost of operation [16], [9], temperature cooling [12] and thermal fairness [5], [4]. Several researchers have also identified the need for optimizing the supply temperature of water in district heating systems [6], [18], [13]. In another body of work [10], [19], [11], the authors propose a multi-agent systems framework for demand side management in DHC networks. In these papers, a modified or *fake* ambient temperature is used as a DR signal to mitigate the problems of peak load in a DHC network. More recently, in [7], the authors propose a framework DHC network operational cost where buildings share resources such as CHP generators, storage elements and renewable power generators.

Broadly speaking, the hierarchical nature of DReAM is similar to the ones studied in [19] and [11]. However, whereas the authors in [19] focus more on an algorithmic treatment of the multi-agent system architecture for demand side management, we provide a more in-depth mathematical analysis of the proposed DR architecture. In [11], the demand side management in DHC networks is done in a need-based dynamic manner through a sealed bid first price auction process. In contrast, our proposed algorithm bypasses dynamic gaming among agents in the DHC network, gathers the information necessary from downstream consumers (such as comfort preferences) at one shot and subsequently optimizes system operation through a low complexity optimization algorithm without the direct intervention of end-level consumers. Additionally, our proposed DR framework ensures that the comfort preferences of the end-level consumers are respected to a fair degree.

The system model in this work is similar to prior work in [5], [4]. However, unlike in [5] and [4] where authors only considered one building under each substation, we consider a more realistic setting where we have multiple buildings under one substation. This makes the mathematical analysis more complex and we cannot represent the steady state network quantities in closed form as seen in [5] and [4]. Secondly, whereas [5] and [4] focus on the issue of thermal fairness, this work is aimed at minimizing a weighted combination of the cost of power consumption in the DHC network and the overall discomfort incurred by the consumers in the network. The rest of the paper is organized as follows. First, we provide a detailed description of the DHC network model considered in this work. We then explain the DReAM framework. Subsequently, we evaluate the effectiveness of DReAM on a test network comprising of multiple substations (each with multiple buildings) under different scenarios.

2 SYSTEM MODEL

Please refer to Figure 1 for this section. Consider a DHC network with a central heat source consuming $\dot{Q}_{in,network}(t)$ power at time t. Denote the return temperature and supply temperature of water at the central energy source as T_R and T_S respectively. The DHC network feeds a collection of substations (connected in parallel topology), each of which has a primary side (metered by utility) and a secondary side (houses individual buildings). Let $\mathcal{N}_s$ be the set of all substations and the total number of substations be N. Owing to thermal losses during heat transport, the effective supply temperature of water at any substation i is denoted as $T_{PS,i}$ where $T_{PS,i} = T_S - \rho_i$ ($\rho_i > 0$ is the effective thermal temperature loss for substation i). Similarly, if the return water from substation (primary side) i is at temperature $T_{PR,i}$, the loss adjusted effective return temperature from substation i is denoted as $T_{R,i} = T_{PR,i} - \rho_i$. In general, utility companies have a reference chart which prescribes the optimal supply water temperature T_S with respect to the ambient temperature T_∞. In our work, we consider $T_S = f(T_\infty) = a_1 T_\infty + a_2$, where a_1 and a_2 are scalar constants which vary among different utility companies. In the secondary side of any substation i, let $T_{SS,i}$ and $T_{SR,i}$ be the temperature of the supply water and return water respectively. Let $\dot{m}_{P,i}$ and $\dot{m}_{S,i}$ be the mass flow rates of water in primary and secondary side of the substation i's heat exchanger.

2.1 Primary side equations:

Assume $h_{S,i}$ to be the heat exchanger coefficient of substation i. At the substation level, we assume perfect insulation, and hence, by law of conservation of energy,

$$\dot{Q}_{in,i} = \dot{m}_{S,i} C_p (T_{SS,i} - T_{SR,i}) = \dot{m}_{P,i} C_p (T_{PS,i} - T_{PR,i}), \quad (1)$$

where $\dot{Q}_{in,i}$ is the total amount of power being consumed by substation i. Also, the heat exchange equation at the substation level is modeled by the equation,

$$\dot{Q}_{in,i} = h_{S,i} \frac{T_{PS,i} - T_{SS,i} - T_{PR,i} + T_{SR,i}}{\log\left(\frac{T_{PS,i} - T_{SS,i}}{T_{PR,i} - T_{SR,i}}\right)}. \quad (2)$$

Note that equation (3) is nonlinear and to simplify the algebra, we assume a linear equivalent of the same. This is represented in the successive equation,

$$\dot{Q}_{in,i} = h_{S,i}\left(\frac{T_{PS,i} + T_{PR,i}}{2} - \frac{T_{SS,i} + T_{SR,i}}{2}\right). \quad (3)$$

2.2 Secondary side equations:

Let $\mathcal{N}_{b,i}$ denote the set of buildings under substation i. Assume that the effective supply temperature of hot water to these buildings is $T_{SS,i}$. Inside every building, we assume there is a radiator which exchanges the heat of the water with the indoor heating space. Let $h_{R,ij}$ be the radiator heat exchanger coefficient of the j^{th} building connected to the i^{th} substation. The return water temperature from building j is denoted as $T_{SR,ij}$. We assume that a proportional controller is present in every building which attempts to drive the indoor temperature ($T_{z,ij}$) towards a specific set-point ($T_{sp,ij}$) by controlling the mass flow rate ($\dot{m}_{S,ij}$). Note that $\dot{m}_{S,i} = \sum_{j \in \mathcal{N}_{b,i}} \dot{m}_{S,ij}$. The following set of equations can then

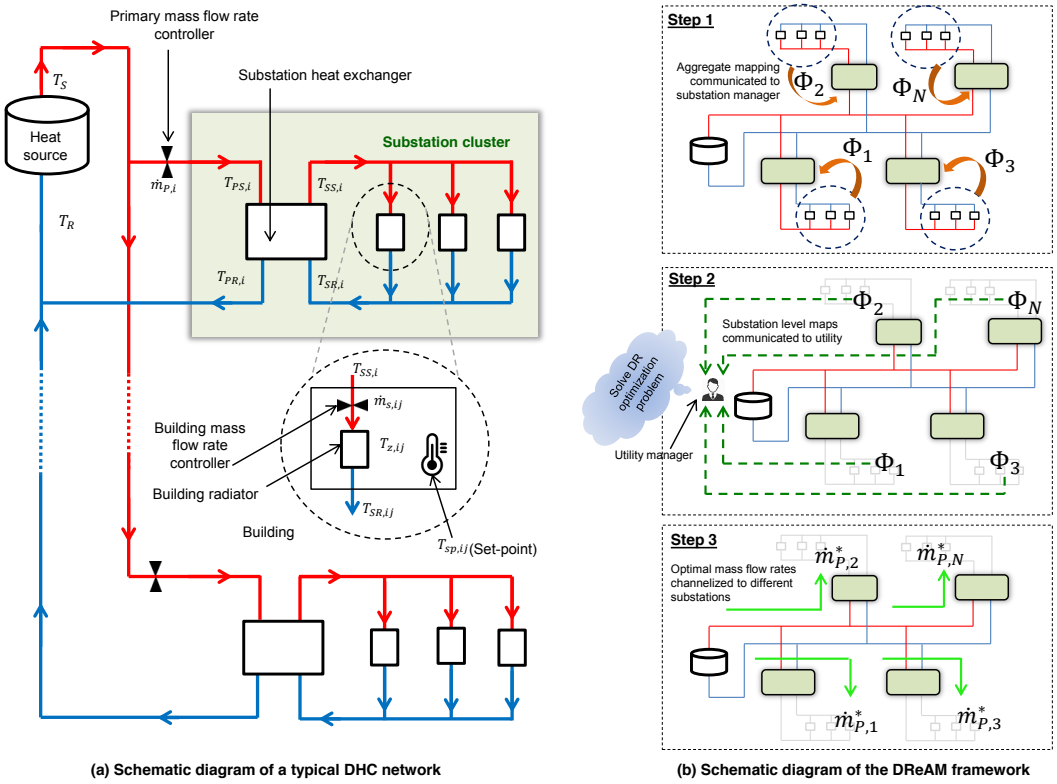

(a) Schematic diagram of a typical DHC network

(b) Schematic diagram of the DReAM framework

Figure 1: (a) Schematic diagram of a typical DHC network with substations connected in parallel and (b) schematic diagram explaining the DReAM architecture.

be written to model the part of the DHC network downstream of substation i.

$$\dot{m}_{S,ij} = \min\left(K_{z,ij}(T_{sp,ij} - T_{z,ij}) + \zeta_{ij},\ \dot{M}^{ub}_{ij}\right), \tag{4}$$

$$\dot{m}_{S,ij}C_p(T_{SS,i} - T_{SR,ij}) = h_{R,ij}\left(\frac{T_{SS,i} + T_{SR,ij}}{2} - T_{z,ij}\right), \tag{5}$$

$$C_{ij}\dot{T}_{z,ij} = \frac{1}{R_{ij}}\left(T_\infty - T_{z,ij}\right) + \dot{m}_{S,ij}C_p(T_{SS,i} - T_{SR,ij}). \tag{6}$$

Equation (4) denotes the proportional control law action for the mass flow rate in building j. Note that the mass flow rate is upper bounded by $\dot{M}^{ub}_{ij}$ which can be interpreted as the valve saturation limit. $K_{z,ij}$ and ζ_{ij} are the proportional controller constants. Equation (5) denotes the heat exchange dynamics (linearized equivalent similar to (3)) between the building radiator and the indoor space. C_p is the specific heat capacity constant of water. Equation (6) governs the indoor zone temperature evolution in building j. R_{ij} and C_{ij} denote the equivalent thermal resistance and capacitance in building j under substation i, respectively. Also, define $\dot{Q}_{in,ij}$ as $\dot{Q}_{in,ij} = \dot{m}_{S,ij}C_p(T_{SS,i} - T_{SR,ij})$ to be the net power consumed by building j in substation i. If there are P_i buildings in substation i, i.e. cardinality of set $\mathcal{N}_{b,i}$ is P_i, then there are P_i equations each of the form (4), (5) and (6) which model all the buildings under substation i. The overall return temperature of water in the secondary side of substation i can now be found out by applying the law of conservation of energy, and is given as,

$$T_{SR,i} = \frac{\sum_{j\in\mathcal{N}_{b,i}} \dot{m}_{S,ij}T_{SR,ij}}{\sum_{j\in\mathcal{N}_{b,i}} \dot{m}_{S,ij}} = \frac{\sum_{j\in\mathcal{N}_{b,i}} \dot{m}_{S,ij}T_{SR,ij}}{\dot{m}_{S,i}}. \tag{7}$$

Note that the total number of equations which model the secondary side of any substation i is $3P_i + 1$.

3 THE DReAM FRAMEWORK

Let $C(\dot{Q}_{in,network})$ be the cost of power consumption for the DHC network. Assume $C(\cdot)$ to be convex in $\dot{Q}_{in,network}$. Let $G_{ij}(T_{z,ij})$ denote the disutility (discomfort) incurred for consumer in building j under substation i at indoor temperature $T_{z,ij}$. Also, define $G_i : \mathbb{R}^{P_i} \to \mathbb{R}$ such that $G_i(T_{z,ij}\forall j \in \mathcal{N}_{b,i}) = \sum_{j\in\mathcal{N}_{b,i}} G_{ij}(T_{z,ij})$ as the *aggregate disutility* of substation i. We assume that the overall network-wide demand response objective of the utility manager is to minimize a weighted cost of power consumption and the aggregate disutility of building consumers subject to the network thermodynamic constraints (as explained in Section 2) by controlling the thermostat set-points for all buildings in the network ($T_{sp,ij}\ \forall i, \forall j$).

Mathematically,

$$\min_{T_{sp,ij}, \forall i \forall j} C(\dot{Q}_{in,network}) + \gamma\Big(\sum_{i \in \mathcal{N}_s} G_i(T_{z,ij}\ \forall j \in \mathcal{N}_{b,i})\Big), \quad (8)$$

$$s.t.\ (1) \text{ and } (3)\ \forall i \in \mathcal{N}_s, (4)-(7)\ \forall i \in \mathcal{N}_s \text{ and } \forall j \in \mathcal{N}_{b,i}. \quad (9)$$

From a computational standpoint, the above problem can be highly resource intensive, especially when the number of buildings is high. The proposed framework (DReAM) tackles this problem by abstracting the entire network at the substation level through a bi-level decomposition technique and then solving the DR optimization problem with the low complexity abstracted network. The exact details of the proposed framework are explained as below.

3.1 Bi-level network decomposition

In order to abstract the portion of a DHC network downstream to a substation, it is important to construct appropriate functional mappings between all downstream secondary side variables with respect to a single secondary side variable that can uniquely explain the variation of the others. The following two results (DReAM Idea 1 and DReAM Idea 2) show how it is indeed possible to (a) decompose the overall DHC network into two levels; a higher level (abstracted at primary side substation level granularity) and a lower level (including all secondary side elements downstream to a substation) linked by an intermediate secondary variable i.e. a linkage variable and (b) a primary side control technique to implicitly achieve desired values for this aforementioned linkage variable.

3.1.1 ***DReAM Idea 1:*** $T_{SS,i}$ ***as the secondary side linkage variable.*** Let us focus on the secondary side equations, and consider steady state of operation. The steady state equivalent of (6) can be found by setting $\dot{T}_{z,ij} = 0$, which gives,

$$\dot{m}_{S,ij} C_p (T_{SS,i} - T_{SR,ij}) = \frac{1}{R_{ij}}\Big(T_{z,ij} - T_\infty\Big). \quad (10)$$

Now, note that (4), (5), (7) and (10) together consists of a system of $3P_i + 1$ equations that together denote the steady state model of the entire secondary side of substation i. Now assume that the $T_{SS,i}$ is fixed to a certain value. The unknown variables (each in their steady state) are then $\dot{m}_{S,ij}\ \forall j \in \mathcal{N}_{b,i}$, $T_{SR,ij}\ \forall j \in \mathcal{N}_{b,i}$, $T_{z,ij}\ \forall j \in \mathcal{N}_{b,i}$ and $T_{SR,i}$. Clearly, the number of unknowns is $3P_i + 1$. Thus, given a fixed steady state $T_{SS,i}$, known $T_{sp,ij}\ \forall j \in \mathcal{N}_{b,i}$ and a known T_∞, we have a system of $3P_i + 1$ equations and $3P_i + 1$ unknowns that completely specify the secondary side of substation i. This system of equations can now be solved to get the definite steady state values of $\{T_{z,ij}\}_{j=1}^{P_i}$, $\{\dot{m}_{S,ij}\}_{j=1}^{P_i}$, $\{T_{SR,ij}\}_{j=1}^{P_i}$ and the $T_{SR,i}$. Consequently, one can get the relationship of $\dot{Q}_{in,ij} = \dot{m}_{S,ij} C_p (T_{SS,i} - T_{SR,ij})$ for any given $T_{SS,i}$. Thus, we understand that for a substation, given the $T_{sp,ij}$ for all buildings it houses, and the T_∞, one can establish the following mappings (under steady state):

- $\dot{Q}_{in,i} = \Psi_{1,i}(T_{SS,i})$
- $\dot{m}_{S,ij} = \Psi_{2,i}(T_{SS,i}),\ \forall j \in \mathcal{N}_{b,i}$,
- $T_{z,ij} = \Psi_{3,i}(T_{SS,i})\ \forall j \in \mathcal{N}_{b,i}$,
- $T_{SR,ij} = \Psi_{4,i}(T_{SS,i})\ \forall j \in \mathcal{N}_{b,i}$,
- $T_{SR,i} = \Psi_{5,i}(T_{SS,i})\ \forall j \in \mathcal{N}_{b,i}$,
- $G_i = \Psi_{6,i}(T_{SS,i})$

Denote $\Phi_i = \{\Psi_{1,i}, \Psi_{2,i}, \ldots, \Psi_{6,i}\}$. Substations usually have a manager (operator who oversees the energy exchange process between the consumers in the substations and the utility side). These substation managers are expected to be aware of their respective Φ_i over the appropriate ranges of T_∞ and $T_{SS,i}$. They also typically have a benchmark curve (function of the ambient temperature) for maintaining certain specific $T_{SS,i}$ at the secondaries which guarantee satisfactory energy delivery to the substation. For substation i, let us denote this reference curve as $T_{SS,i} = b_{1,i} T_\infty + b_{2,i}$, where $b_{1,i}$ and $b_{2,i}$ are scalar constants unique to substation i.

3.1.2 ***DReaM Idea 2:*** $\dot{m}_{P,i}$ ***as the primary side control input.*** To ensure a resultant $T_{SS,i}$ under steady state, there must be a knob which the utility can control from the primary side. The primary mass flow rate i.e. $\dot{m}_{P,i}$ can be treated as such a knob. To see this, we now focus on the primary side equations. Assume that the secondary side parameters have already been determined corresponding to a certain $T_{SS,i}$ (say $T^*_{SS,i}$). Now, given a certain steady state $T^*_{SS,i}$, a resultant $T^*_{SR,i}$ and a known $T^*_{PS,i}$ (from the utility chart), the utility can solve using (3), the corresponding $T^*_{PR,i}$. Subsequently, one can also get the resultant $\dot{m}^*_{P,i}$ from (1). Inversely, one can say that if the utility side channels $\dot{m}^*_{P,i}$ on the primary side to the substation i, it would result in $T^*_{SS,i}$ on the secondary side circuit under convergence to steady state conditions.

3.2 The DReAM optimization formulation

It has already been reported in previous papers such as [5] and [4] that optimizing the objective functions such as those in (8) subject to dynamic network constraints for the entire look ahead window may be resource intensive and complex. Therefore, a receding window based optimization technique based on steady state assumptions (similar to the ones in [5] and [4]) is proposed. Under such a paradigm, the entire look ahead is divided into K time slots. For the k^{th} slot, the utility's optimization problem can be stated as,

$$\begin{aligned} \min_{T_{SS,i}(k), \forall i} \quad & C(\dot{Q}_{in,network}(k)) + \gamma\Big(\sum_{i \in \mathcal{N}_s} G_i(T_{z,ij}(k)\ \forall j \in \mathcal{N}_{b,i})\Big), \\ s.t. \quad & \Phi_i, \forall i \in \mathcal{N}_s. \end{aligned}$$

Once $[T^*_{SS,1}(k), \ldots, T^*_{SS,N}(k)]^T$ is determined by solving the above optimization problem, the utility manager can then use equations (1) and (3) to get the corresponding optimal control input vector i.e. the vector of optimal primary mass flow rates to be channelized to the individual substations in time slot k. We repeat this in a receding horizon policy to cover the entire look ahead window under consideration i.e. for all k such that $k \in \{1, 2, \ldots, K\}$. Note that Φ_i encapsulate all downstream information of substation i and once reported, it can be reused by the utility to solve the optimization problem throughout the look ahead window. The mappings may be re-estimated at any point of time to reflect the updated network conditions, in case they vary over time.

Thus, through the DReAM framework, the intractable optimization problem of (8) and (9) that was defined at a building level granularity (with decision space dimensionality $\sum_{i=1}^{N} P_i$) has now been reduced to a more tractable, computationally efficient variant, for which the dimensionality of the decision space is also significantly reduced (reduced dimensionality is just N). A unified stepwise representation of the DReAM framework can be seen in Figure 1.

4 NUMERICAL STUDY

In this section, we provide a suite of numerical examples and studies which highlights the effectiveness of DReAM on a simple test network having four substations, each having 3 buildings connected to it. We also consider that the cost of power at the central source is convex in the power obtained. Owing to space constraints, the details of this setup have been moved to [2].

We first study the steady state substation level mappings (reported to the central utility in step 1 of DReAM) for a particular substation. For brevity, we show the mappings for substation 2 only. Similar mappings can also be stablished for all other substations. Note that in this study, we show the mappings for five different ambient temperatures for ease of exposition. The mappings are assumed to be available for the entire relevant range of ambient temperatures over which DHC network operations are conducted. In Figure 2, we study how the steady state power consumption and the steady state indoor temperature of a building in that substation varies with changing the T_{SS} of that substation. We observe that as the T_{SS} is increased, the amount of power consumption also increases in the substation. This leads to higher indoor zone temperatures. After a point, as the indoor zone temperatures nears its desired set-point, the power consumption also saturates at some level. Also note that a lower ambient temperature requires a higher T_{SS} and hence a higher $\dot{Q}_{in}$ to maintain the indoor zone temperature at a given constant level.

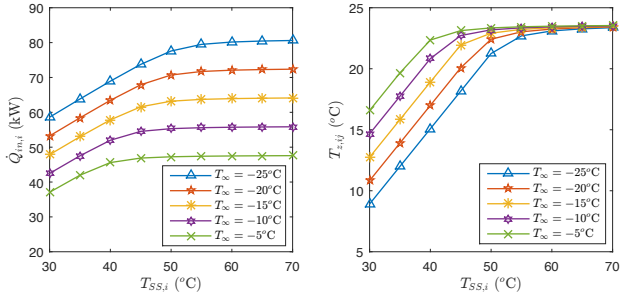

Figure 2: Variation of substation power consumed (and corresponding indoor zone temperature achieved in one building of the substation) with respect to secondary circuit supply water temperature.

In Figure 3, we study the effect of varying T_{SS} on the secondary mass flow rates and the utility side primary mass flow rate. We observe that a lower T_{SS} implies a lower steady state temperature and hence, a higher steady state secondary mass flow rate. Also, due to saturation limit on the secondary mass flow rate controllers, we see that below a certain threshold T_{SS}, the secondary mass flow rates saturates to the valve limit point under steady state operations. Also note that this T_{SS} threshold is higher for a lower ambient temperature. We also observe that in order to maintain a higher T_{SS} at a substation secondary side, one must channelize a higher $\dot{m}_P$ (primary flow rate) to that substation's primary side. Similar mappings can be obtained for all other secondary side and primary side quantities with respect to the T_{SS} but have not been included here for the sake of brevity.

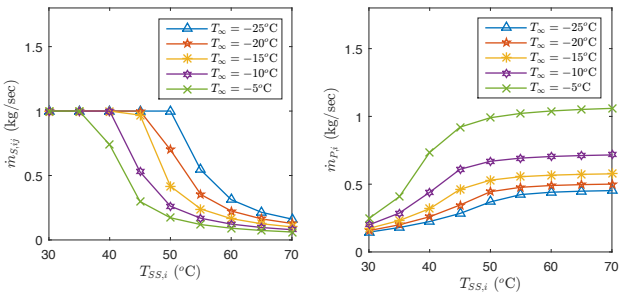

Figure 3: Variation of secondary mass flow rate of one building and primary mass flow rate (of the substation) with respect to secondary circuit supply water temperature.

With the substation maps constructed and reported to the utility manager, we now perform a set of experiments in which we study the effectiveness of DReAM (specifically the effectiveness of step 2 in DReAM) over a 12 hour window. The variation of ambient temperature in this 12 hour window is given in [2]. We choose $\gamma = 0.02$ for our initial experiments.

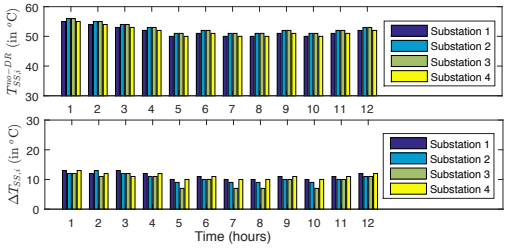

Figure 4: Top: The variation of the supply temperature in the secondary when there is no DR. Bottom: The specific $\Delta T_{SS,i}$ for the substations over the 12 hour window.

In Figure 4, we report the without-DR $T_{SS,i}$ for each substation along with the effective DR signal (difference between the pre and post DR steady state $T_{SS,i}$ values). We see that different substations are taken control by different extents in each of the 12 hours of the selected time window.

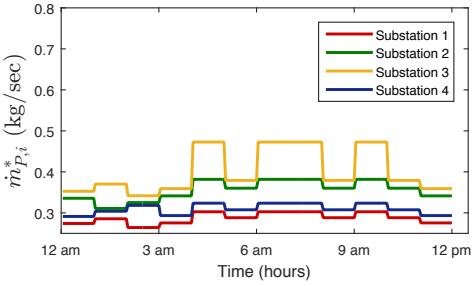

Figure 5: The variation of post-DR optimal primary mass flow rates in each of the four substations over the 12 hour window which is chosen for the case study.

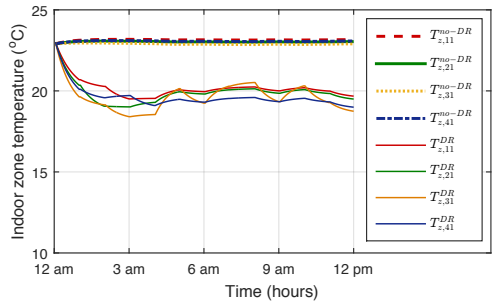

Figure 6: The variation of indoor zone temperature profiles (both without DR and with DR) of one building from each of the four substations over the 12 hour window which is chosen for the case study.

In order to achieve the required $T_{SS,i}$ as deemed fit by the demand response algorithm, the necessary control inputs (i.e. the optimal primary mass flow rates) are computed and have been subsequently plotted for the 12 hour window in Figure 5. We observe that the amount of mass flow rate to be channelized to a substation bears a degree of positive correlation with the level of insulation of buildings, for the buildings under that substation. Substation 3 has the least insulated building and clearly requires a comparatively higher flow rate (than the other substations) for maintaining the indoor temperature of its buildings at the post-DR optimal values.

We now observe the indoor zone temperature profiles of the buildings under the substation under conditions of DR as well as when no DR is effected. We plot the indoor zone temperatures for one building from each of the 4 substations (for ease of exposition) in Figure 6. Clearly, when there is no demand response, the indoor zone temperatures in all buildings hover around their desired set-points i.e. 23°C. With demand response, the indoor zone temperatures are seen to become lower, hovering around 20°C. This is because, with demand response, a curtailment of power input is made to each of the four substations. Thus, there is inadequate energy available for the buildings to ramp up their temperatures to their desired set-point.

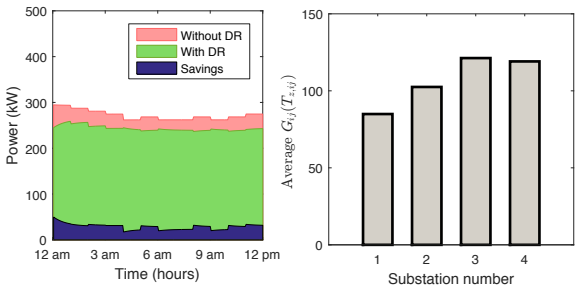

Figure 7: Left: Power consumption by the total DHC network (a) without DR (b) with DR. Also shown is the actual power savings effected by DR. Right: The average disutility $G_{ij}(T_{z,ij})$ incurred by one building in each of the four substation during the DR implementation ($\gamma = 0.02$).

Define the average disutility of building j in substation i as $G_{ij,avg} = \frac{1}{T}\int_0^T G_{ij}(T_{z,ij}(t))dt$. In Figure 7, we represent the power consumption in the total DHC network, under conditions of demand response and when there is no demand response. An interesting point to observe is that through demand response, the post-DR power consumption is brought down to hover around 240 kW during 2 am to 12 pm. Beyond 240 kW, the cost of power usage rises steeply [2] and due to the relatively low value of γ the optimization tries to maintain the energy consumption at or below 240 kW. We also observe from the plot (right side) in Figure 7 that in this chosen DHC network, the buildings downstream of substation 3 incur the maximum disutility. This can be attributed to the comparatively lesser insulation level of the buildings of substation 3, coupled with the fact that substation 3 is located comparatively farther away from the central heat source.

Next, in Figure 8, we report the net steady state disutility of all consumers i.e. $\sum_{i\in\mathcal{N}_s} G_i$ and the steady state costs of net power consumed by the DHC network in the different slots under varying levels of γ. We can thus conclude that as γ increases, i.e. the DHC utility company gives more importance to consumer comfort, the greater is its expenditure of the utility company to secure the energy at the source and lesser is the DR efficacy.

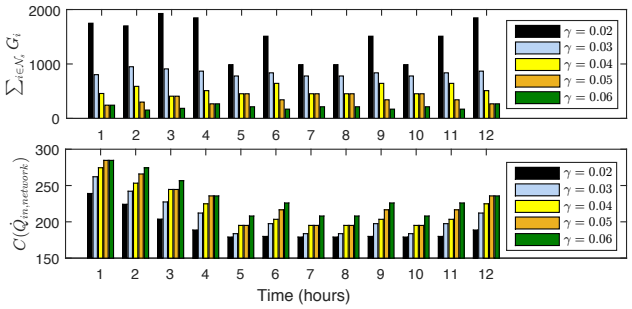

Figure 8: Effect of γ on the network wide consumer disutility and the cost of power consumption across all the time slots of the selected look ahead window.

5 DISCUSSION AND FUTURE WORK

In this paper, we propose a DR framework called DReAM for DHC networks. In the first of these 2 steps, substation managers abstract the consumer side information and the portion of the network which is downstream to that substation. These abstracted models are of low complexity and are reported to the central utility manager. In the second step, the central utility manager employs these abstracted models to devise appropriate DR strategies for the entire network in an iterative, receding horizon method.

In future work, we will investigate the existence of appropriate pricing functions which can serve to bring about coordination in energy usage of the consumers in a decentralized manner. Secondly, in this work, we assume that the substation manager is aware of the building thermal parameters, the building radiator heat exchanger constants and the proportional controller constants for all the consumers under its purview. Realistically, a data driven technique may be needed to mine these building parameters as well which merits an independent investigation subject to data availability.

REFERENCES

[1] 2013. Euroheat and Power (DHC Country by Country survey 2013). *www.dhcplus.eu/wp-content/uploads/2012/02/2010-report.pdf* (2013).

[2] 2017. DReAM: Demand response architecture for multi-level district heating and cooling networks. *[Online]. https://www.dropbox.com/s/y8fdopvtkts6vwi/technicalreport.pdf?dl=0* (2017).

[3] 2017. Steam service. *https://www.coned.com/en/commercial-industrial/steam* (2017).

[4] S. Bhattacharya, V. Chandan, V. Arya, and K. Kar. 2016. Fairness based Demand Response in DHC Networks using Real Time Parameter Identification. In *2016 IEEE International Conference on Smart Grid Communications (SmartGridComm)*. 32–37.

[5] S. Bhattacharya, V. Chandan, V. Arya, and K. Kar. 2016. Thermally-fair demand response for district heating and cooling (DHC) networks. In *Seventh International Conference on Future Energy Systems (e-Energy)*. 154–164.

[6] Stefan Grosswindhager, Andreas Voigt, and Martin Kozek. 2012. Predictive Control of District Heating Network using Fuzzy DMC. In *2012 International Conference on Modelling, Identification and Control*. 241–246.

[7] D. Ioli, F. Alsone, S. Schuler, and M. Prandini. 2016. A compositional framework for energy management of a smart grid: a scalable stochastic hybrid model for cooling of a district network. In *12th IEEE International Conference on Control & Automation (ICCA)*. 389–394.

[8] Pengfei Jie, Neng Zhu, and Deying Li. 2015. Operation optimization of existing district heating systems. *Applied Thermal Engineering* 78 (January 2015), 278–288.

[9] Z.X. Jing, X.S. Jiang, Q.H. Wu, W.H. Tang, and B. Hua. 2014. Modelling and optimal operation of a small-scale integrated energy based district heating and cooling system. *Energy* 73 (July 2014), 399–415.

[10] C. Johansson, F. Wernstedt, and P. Davidsson. 2010. Deployment of Agent Based Load Control in District Heating Systems. In *First workshop on Agent Technology in Energy Systems (ATES)*.

[11] C. Johansson, F. Wernstedt, and P. Davidsson. 2012. Smart Heat Grid on an Intraday Power Market. In *Third workshop on Agent Technology in Energy Systems (ATES)*.

[12] Maunu Kuosaa, Martin Aalto, M. El Haj Assad, Tapio Makila, Markku Lampinena, and Risto Lahdelmaaa. 2014. Study of a district heating system with the ring network technologyand plate heat exchangers in a consumer substation. *Energy and Buildings* 80 (May 2014), 276–289.

[13] P. Lauenburg and J. Wollerstran. 2013. Adaptive control of radiator systems for a lowest possible districtheating return temperature. *Energy and Buildings* 72 (December 2013), 132–140.

[14] H. Lund, B. Moller, B.V. Mathiesen, and A. Dyrelund. 2010. The role of district heating in future renewable energy systems. *Energy* 35 (January 2010), 1381–1390.

[15] Henrik Lund, Sven Werner, Robin Wiltshire, Svend Svendsen, Jan Eric Thorsen, Frede Hvelplund, and Brian Vad Mathiesen. 2014. 4th Generation District Heating(4GDH) Integrating smart thermal grids into future sustainable energy systems. *Energy* 68 (March 2014), 1–11.

[16] Marouf Pirouti, Audrius Bagdanavicius, Janaka Ekanayake, Jianzhong Wu, and Nick Jenkins. 2013. Energy consumption and economic analyses of a district heating network. *Energy* 57 (March 2013), 149–159.

[17] B. Rezaie and Mark A. Rosen. 2012. District heating and cooling: Review of technology and potential enhancements. *Applied Energy* 93 (2012), 2–10.

[18] H. I. Tol and S. Svendsen. 2012. Operational Planning of Low-Energy District Heating Systems Connected to Existing Buildings. In *2nd International Conference on Renewable Energy: Generation and Applications*.

[19] F. Wernstedt, P. Davidsson, and C. Johansson. 2007. Demand Side Management in District Heating Systems. In *6th ACM International Joint Conference on Autonomous Agents and Multiagent Systems (AAMAS)*. 272–278.